

The COP KIN[®] System Part I: Fundamentals and Mathematical Modelling

Andreas Filzwieser, Johann Kleicker, Kevin Caulfield and Stefan Wallner
RHI AG
Wienerbergstraße 11
A-1100 Vienna, Austria
andreas.filzwieser@rhi-ag.com

ABSTRACT

Today gas stirring systems are a standard technique in the steel industry and also in the non ferrous industry such systems are becoming more widely used. Although the operations are varied, for example the stirring gas can be used as a reactive gas being part of the metallurgical process or as an inert gas using the rising gas bubbles for agitation only, the underlying principles are always the same. Which effect turns out to be the most important depends on the process and the requirements of the user. The optimal number and position of plugs in the furnace is strongly influenced by the aim of the purging system. For example there is a large difference if an efficient agitation is required or if a preferential movement of the slag to the slag skimming door is required. For an optimized arrangement of all plugs used in a furnace a mathematical modelling approach - the CFD Computational Fluid Dynamics method - is used for each application.

INTRODUCTION

Today, more than 30 years after the first use of a gas stirring system in transport ladles in the steel industry, different type of plugs – porous plugs, multi hole plugs or single pipe plugs – are in use in many different furnaces.

In the steel industry bottom gas purging is standard not only in ladles but also in converters and electric arc furnaces, whilst in the non ferrous industry gas stirring systems are used in -

- Melting furnaces (Al)
- Holding furnaces (Al, Cu)
- Anode furnaces (Cu)
- Peirce Smith Converters (Cu)
- Casting furnaces (Al)
- Ladles (Non ferrous alloys)
- Launderers (Al, Cu)

Many different gases or gas mixtures are available, for example nitrogen, argon, air, nitrogen/air, nitrogen/hydrogen, argon/chlorine or nitrogen/argon.

Even though reasons for using a bottom gas stirring system could be different depending on the furnace and process and on the gas used (inert gas or process gas), in general the following are the main reasons for using such a system -

a) Thermal and analytical homogenization of the molten bath

Due to the agitation effect of the purged gas bubbles the convection in the bath and therefore also the heat transfer is increased and a uniform bath temperature and chemical analysis is achieved for the whole process. Further advantages are:

- ✓ reduction of fuel and auxiliary material consumption
- ✓ decreased slag overheating
- ✓ decreased refractory wear
- ✓ uniform chemical purity
- ✓ prevention of coatings

b) Increased surface layer between slag and metal bath

The advantages which are obtained by an increased surface layer between slag and metal bath due to a higher relative movement between slag and bath surface driven by the agitation are -

- ✓ decreased boundary layer
- ✓ increased diffusion-controlled reaction
- ✓ increased metal recovery
- ✓ decreased highly-oxidized slag

c) Inert gas bubbles in the molten bath

The amount of dissolved gas in a liquid is a function of the atmospheric gas partial pressure above the liquid. The partial pressure for CO or SO₂ for example is zero in a inert gas bubble and this fact leads to following:

- ✓ decreased partial pressure for SO₂
- ✓ decreased partial pressure for H₂O
- ✓ decreased partial pressure for CO
- ✓ system reaches equilibrium more quickly

d) Process gas in the molten bath from the bottom

Once again the agitation and improved mixing of the bath is the reason for -

- ✓ increased efficiency of process gas
- ✓ system reaches equilibrium more quickly

Not all effects are as important and during the process the relative importance of any effect could change. But to determine the optimal number and position of plugs in a furnace four points have to be taken into consideration -

- an efficient agitation of the bath
- an efficient distribution of gas bubbles in the whole bath
- an increased relative movement between slag and metal bath
- a preferential movement of slag to the slag skimming door during slag skimming.

To do this work the RHI Non Ferrous Metals Engineering Group use the commercial CFD (computational fluid dynamics) code FLUENT.

This modelling work is one aspect of our latest standardised gas stirring system – the COP KIN[®] System. More information concerning the COP KIN[®] System is given in the paper “The COP KIN[®] System Part II: Performance and benefits – a worldwide overview”.

Fundamentals

Following is a short synopsis of the existing literature concerning gas bubbles in a molten bath.

Bubble Diameter

The bubble diameter is in general a function of the surface tension of the pore with respect to the nozzle diameter and the gas throughput (capacity). With increasing gas throughput, the formation frequency and the size of the bubbles are also increasing. If the gas velocity increases dramatically, a gas stream shoots into

the liquid and disintegrates into a bubble swarm (there are different flow fields in conjunction with the gas flow rate at the input of gas into fluids). With low gas throughput, single bubbles are formed at the openings, whose size are directly related to the characteristics of the system (pore size, metal, pressure and viscosity of the fluid).

The bubble size remains constant with increasing gas supply until a critical level, whilst the formation frequency of the bubbles is changing. Above this critical level, bubble size changes whilst the bubble formation frequency changes. The size of the primary bubble depends predominantly in this situation on the gas flow rate.

Besides the gas flow rate, the distance to the gas flow openings is also critical due to the possibility of a small pore to channel distance causing the escaping gas bubbles to coagulate. In the case of a higher flow rate, a coalition of the gas bubbles in the vertical direction will occur. The field of single gas bubbles will change to a field of a compact gas-stream (“jetting”).

Purging plugs with increased porosity show at increasing gas pressure an increased diameter of the escaping gas bubbles until a build up of a so-called “big bubble” occurs. In this case, the gas stream escapes, not at once, but with a pulsating effect, causing a back attack into the purging plug surface (“back attack effect”). For purging plugs with a reduced porosity, this effect could not be observed, but instead, with increased flow rate, single bubbles of a high specific surface are observed (1).

Depending on the Reynolds number, different bubble diameters occur. The significance and units of the single variables are shown following.

According to (2) -

- for $Re < 500$
$$d_B = \sqrt[3]{\frac{6 \cdot d_0 \cdot S}{g \cdot (r_L - r_G)}} \quad (1-1)$$

- for $500 = Re = 2100$
$$d_B = 0,046 \cdot \sqrt{d_0} \cdot \sqrt[3]{Re_0} \quad (1-2)$$

According to (1) -

- for $Re > 5000$
$$d_B \cong 1,3 \cdot \frac{\sqrt[5]{Q^6}}{\sqrt[5]{g^3}} \quad (1-3)$$

Shape of gas bubbles

Parameter which describes the movement of the gas bubbles (2) -

- Reynolds-Number:
$$Re_B = \frac{d_B * U * \mathbf{r}_L}{\mathbf{m}_L} \quad (1-4)$$

- Weber-Number:
$$We = \frac{d_B * U^2 * \mathbf{r}_L}{\mathbf{s}} \quad (1-5)$$

- Eotvos-Number:
$$Eo = g * d_e^2 * \frac{(\mathbf{r}_L - \mathbf{r}_G)}{\mathbf{s}} \quad (1-6)$$

- Morton-Number:
$$Mo = \frac{g * \mathbf{m}_L^4}{\mathbf{r}_L * \mathbf{s}^3} \quad (1-7)$$

Referring to the references (1), (3), (4) and others, the following general statements can be made (Figure 1) -

- Small Reynolds-Number $Re < 1$. Many small bubbles are shown.
- Large Reynolds-Number $Re > 1000$ and large Eotvos-Number $Eo > 50$. A half sphere bubble is shown. Build-up of big bubbles within fluids of low to intermediate viscosity.
- At intermediate range figures for Re and Eo , sickle shaped bubbles are shown.

At intermediate figures for Re and Eo , bubbles with an elliptical shape are shown, which are the most suitable for a circular movement.

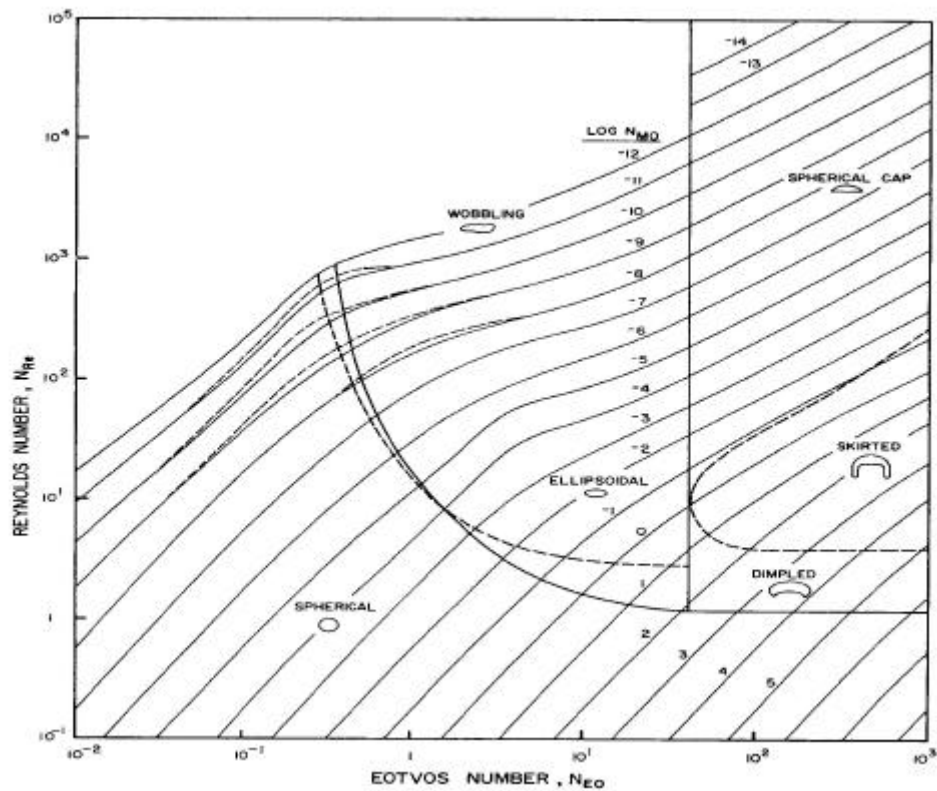


Figure 1 - Bubble shape as a function of Reynolds and Eotvos-Numbers (2).

Ascent velocity of the bubble

Numerical calculations of the ascent velocity in comparison with the bubble diameter according to (2) are shown in Table I.

Table I - Ascent velocity according to (2).

Bubble size (cm)	Reynolds-Number	Ascent speed U_t
$d_B < 0,2$	$Re_B < 2$	$U_t = \frac{d_B^2}{18 * m} * g * (r_L - r_G) \quad (1-8)$
$0,2 < d_B < 0,4$	k.A.	$U_t = \frac{d_B^2 * g}{12 * m} \quad (1-9)$
$d_B > 1$	$Re_B > 1000$	$U_t = 0,79 * \sqrt{g} * \sqrt[6]{V_B} \quad (1-10)$

CFD-Modelling

Theory

The numerical calculation of fluid flow or heating- and temperature-distribution is possible, if the physical laws can be transformed into mathematical equations, usually into differential equations.

Each single differential equation is linked to a certain conservation law and consists of one physical value as a dependent variable. It is assumed that the different factors influencing the physical value are in equilibrium.

The dependent variable of these differential equations is used as a specific value, that is, it is calculated from one device volume. Examples of these are the velocity (momentum per device volume), the mass- or rule of agitation and the specific enthalpy/energy. The temperature that is often given as a dependent variable is not a specific value, because it is combined in a fundamental equation with the energy/enthalpy equation.

The single terms of a differential equation show the influence of an imaginary unit volume. An example of the continuity equation, the conservation of mass will be calculated from a two dimensional field.

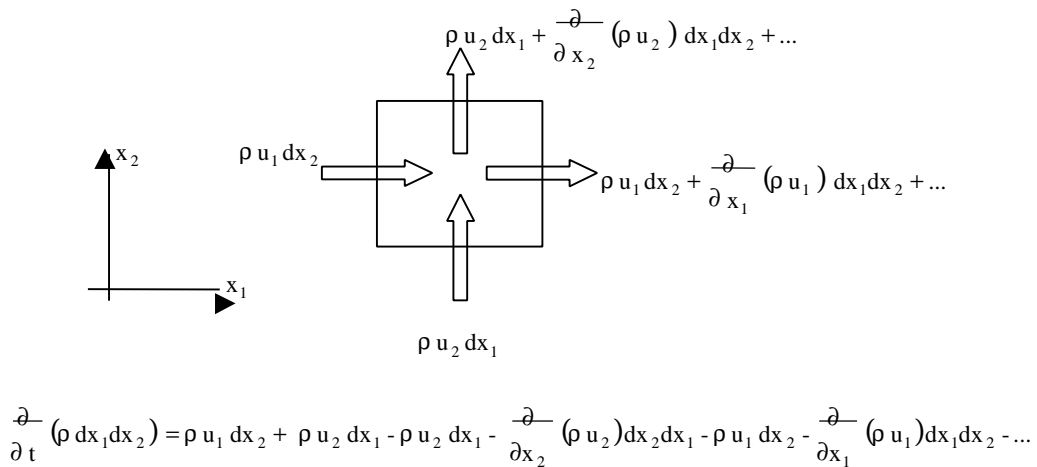


Figure 2 - Two dimensional area field (5).

Looking at Figure 2 an element in the two dimensional space with the edge dx_1 and dx_2 is shown. The continuity equation is the result of the calculation in both directions x_1 and x_2 with consideration of the change as a function of time of the density – according to the mass input per volume in kg/m^3 .

$$\frac{\partial \rho}{\partial t} + \frac{\partial}{\partial x_1} (\rho u_1) + \frac{\partial}{\partial x_2} (\rho u_2) = 0 \quad (2)$$

The differential equation which describes the conservation of momentum for one direction of one volume element of a Newton's fluid, can be calculated in a similar way as previously described. With u for the velocity vector and u_1 as the velocity component in x_1 -direction it can be described as -

$$\frac{\partial(\rho u_1)}{\partial t} + \text{div}(\rho u u_1) = \text{div}(\mu \text{grad} u_1) - \frac{\partial p}{\partial x_1} + B x_1 \quad (3)$$

with μ as the viscosity, p the pressure and B as "body force" in x_1 -direction, for example the gravitational acceleration. The individual parts of this differential equation describe the different kinds of momentum transportation. The first part of the term $\partial(\rho u_1) / \partial t$ corresponds to the rate of momentum exchange (changing the velocity) per time interval, the term $\text{div}(\rho u u_1)$ the convective flow of the momentum, which will be transformed due to the general velocity field u . The term $\text{div}(\mu \text{grad} u_1)$ indicates the diffuse part of the momentum transport, with $\mu \text{grad} u_1$ relating to Fick's diffusion law.

The viscosity μ corresponds to the "diffusion coefficient" of the momentum and $\text{grad} u_1$ the differential of the momentum of the volume element. The term $\partial p / \partial x_1$ shows the part of the pressure force to the complete momentum calculation. The momentum conservation equation is referred to as Navies-Stokes-Equation.

The conservation of momentum equation just described operates only in the case of laminar conditions but turbulent flows occur in nearly all technical processes. Only in very special cases and using considerable computing time is it possible to solve unstable turbulent flows. In numerical flow calculations it is common to use time dependent and amalgamated values of the dependent variable, for example velocity, density, etc.

For these calculations it is useful to consider that on average a fast and hazardous fluctuation will occur.

In the equation of conservation the current variables on a volume element through the sum of the ensemble calculated values $\langle u \rangle$ and a deviation u' of the calculated value replaced, for example B for the velocity component u -

$$u = \langle u \rangle + u' \quad (4)$$

The correlation of the velocity fluctuation is not known and therefore it must be calculated with a turbulence model. This kind of solution of the equation system is known as "closing the system". In this case it is important that the apparent transverse strain is mainly caused by the larger turbulence conglobes. These large turbulence conglobes give rise to vortex filament extension and in the case of the shear instability of the flow their energy changes to a smaller whirl, until the velocity gradient of the smallest turbulence elements is very steep, so that it is completely transformed into the inner energy.

These transports of energy in the turbulence energy spectrum to larger wave numbers will be known as turbulence energy cascades.

The feeder of energy into these cascades is not dependent on the viscosity. It will take place through transmission of energy of the average movement of the apparent shearing strain on the large turbulence elements. This energy will be given from one small turbulence element to the next until dissipation occurs. This is also the reason that the distribution of the average velocity at turbulent flow is less dependent on the Reynolds number, although the energy loss is caused by the viscosity.

In the process of going through the energy cascade the information of direction of the velocity will be lost. This means that the fluctuation energy during the cascade will be distributed in all directions. The smallest turbulence elements are isotropic. This is common for turbulent flows with large velocity gradients or not twist used rotating flows. These flows are known as local isotropic.

The dependent variables ϕ must be transformed into an average value $\langle\phi\rangle$ and the fluctuated component ϕ' -

$$\phi = \langle\phi\rangle + \phi' \quad (5)$$

For a static stationary flow ϕ is the temporal average:

$$\langle\Phi(x_0)\rangle = \lim_{t_0 \rightarrow \infty} \frac{1}{2 \cdot t_0} \int_{t=-t_0}^{t=t_0} \phi(x_0, t) dt \quad (6)$$

Many different turbulence models are used. For practical and technical purposes the so-called k- ϵ -Model from Harlow and Nakayama (5) will be used. The k- ϵ -Model solves two more partial differential equations for the turbulent kinetic energy k -

$$k = \frac{\overline{u_i^2}}{2} \quad (7)$$

and their dissipation ϵ -

$$e = C_m^{3/4} \frac{k^{3/2}}{l_t} \quad (8)$$

In the equations which are described l_t is for a characteristic turbulent whirl length. For a deeper understanding of this field it is necessary to read the special literature.

Examples

Mixing time and agitation

Rama Rao and Baird (6) investigated in an 87 cm diameter horizontal cylindrical water tank the influence of plug arrangements on mixing time. It was shown (by a video) that using an equally-spaced row of plugs along the tank axis the mixing from one end of the tank to the other one takes approximately 17 minutes. With an uneven spacing between the plugs it was possible to mix the whole tank in not more than 4 minutes. The reason for this was that using the equally-spaced rows single symmetrical cells of the same fluid flow behaviour occur and mixing in the horizontal direction is poor. Using uneven arrangements the area of influence from one single plug is increased.

To verify the mathematical model and to convince customers this water model was completely recalculated and for marketing purposes a CD and also movies from the CFD modelling work were prepared. The comparison of mixing time for different plug arrangements with the movies shows a very good correspondence.

As shown in Figure 3, using six equally-spaced plugs also the velocity distribution on the top shows single similar cells, whilst on the other hand also using six plugs but in two groups the mixing time was just 4 minutes in comparison with 17 minutes previously.

In Figure 4 a cross section through an anode furnace is shown. For all parameters of course the “true” values were chosen such as bath temperature, viscosity of blister copper, viscosity of slag, metal and slag height, flow rate for the poling gas through the poling blocks (it is seen on the right of each picture), flow rate of the purged gas through the plug (left picture only), correct dimension of the furnace and so on. Looking more closely at this calculation then it is seen that the influence of the poling gas is of great importance but the mixing occurs in a very small area only. In the middle of the furnace the velocity of the blister is less than 10 cm/s whereas the blister velocity in the furnace equipped with a porous plug is greater than 60 cm/s.

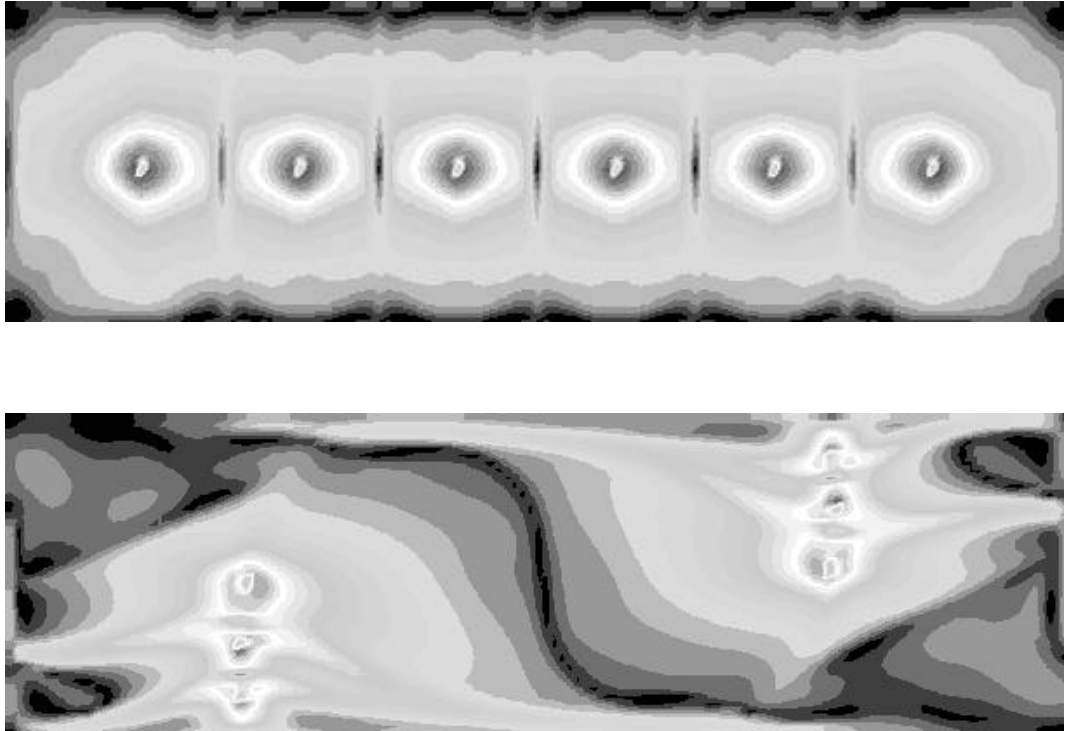


Figure 3 - Velocity distribution on the surface, $v_{\max} = 0.40$ m/s, $v_{\min} = 0.00$ m/s, for two different plug arrangements.

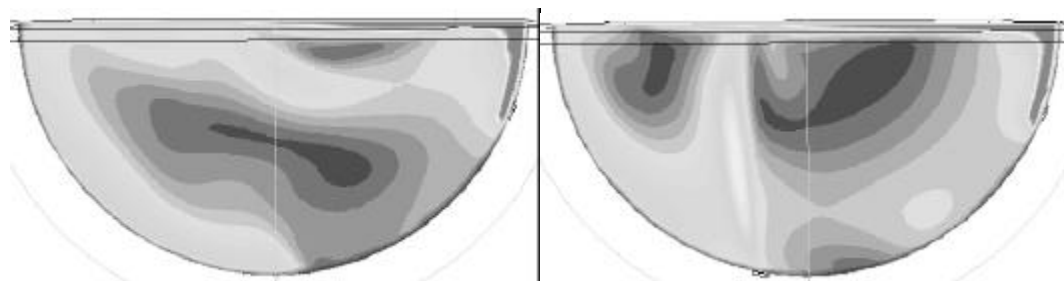


Figure 4 - Left: Anode furnace with porous plug; Right: Anode furnace without plug; $v_{\max} = 1.0$ m/s , $v_{\min} = 0.0$ m/s

Temperature distribution

The calculation of the temperature gradient in the bath for a 320 t/charge anode furnace without a purging system was 17°C. For the same furnace calculated with purging elements the temperature difference in the whole bath was 3°C.

In Figure 3 one can see that without using a stirring system layers of the same temperature occur and thermal homogenisation in the bath is poor. The difference between the top layer and the layer in the bottom was 17°C. In Figure 4 one can see that due to the stirring effect the homogenisation is much better and the temperature difference in the whole bath is just 3°C.

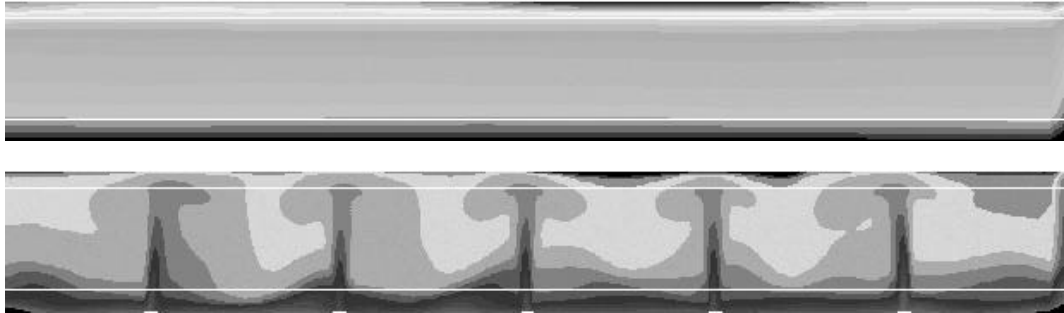


Figure 4 - Temperature distribution in a 320 t anode furnace.

CONCLUSIONS

To determine the optimal numbers and positions of purging plugs is an essential aspect of an efficient gas stirring system. One of the most important features of the COP KIN[®] system is the ability to conduct modelling work using CFD methods.

REFERENCES

1. J. Szekely, Fluid Flow Phenomena in Metals Processing, Academic Press, New York, 1979.
2. J.F. Davidson and D. Harrison, Fluidized Particles, Cambridge University Press, London and New York, 1963.
3. W.L. Habermann and R.K. Morton, "David Taylor Basin Model Report", No. 802, U.S.Dept. of Naval Research, Washington D.C, 1953.
4. V. Levich, Physicochemical Hydrodynamics, Prentice Hall, Englewood Cliffs, New Jersey, 1962.
5. F. Harlow and P. Nakayama, "Transport of Turbulence Energy Decay Rate", Report LA-3845, Los Alamos Science Lab., University of California.
6. N.V. Rama Rao and M.H.I. Baird, "Optimum Bottom-Stirring in a Horizontal Cylindrical Vessel", The Canadian Journal of Chemical Engineering, Vol. 79, 2001, 689-696.

NOMENCLATURE

A	[cm ²]	Substance exchange surface
D	[cm ² /s]	Coefficient of diffusion
d _o	[m]	Diameter of nozzle
d _B	[m]	Diameter of bubble
d _e	[m]	Diameter of pipe
E _o	[-]	Eotvos number
g	[m/s ²]	Coefficient of gravitation
L	[-]	Coefficient of distribution slag/metal
Mo	[-]	Morton number
p ₀	[Pa]	Pressure above gas bubble outlet
p _{atm}	[Pa]	Atmospheric pressure
p _G	[Pa]	Pressure in gas bubble
p _{met}	[Pa]	Metallostatic pressure
p _x	[Pa]	Pressure in gas bubble at height x
p _s	[Pa]	Surface tension pressure
Q	[m ³ /s]	Volume stream
Re ₀	[-]	Nozzle Reynolds number
Re _B	[-]	Bubble Reynolds number
t	[s]	Time
U	[m/s]	Velocity
U _t	[m/s]	Ascent velocity of bubble
V	[cm ³]	Volume of reaction
V _B	[m ³]	Volume of bubble

V_x	$[m^3]$	Volume of bubble at height x
We	[-]	Webber number
β	$[cm/s]$	Coefficient of mass transfer
β_B	$[cm/s]$	Coefficient for transfer bubble-molten bath
β_G	$[cm/s]$	Coefficient for transfer in gas phase
β_S	$[cm/s]$	Coefficient for transfer in molten bath
ρ_G	$[kg/m^3]$	Gas density
ρ_L	$[kg/m^3]$	Fluid density
d_D	$[cm]$	Thickness of diffusion boundary layer
s	$[N/m]$	Surface tension
μ	$[m^2/s]$	Viscosity